The $A\,^6\Sigma^+$-$X\,^6\Sigma^+$ transition of CrH, Einstein coefficients, and an improved description of the A state

Charles W. Bauschlicher, Jr.[a)]
Mail Stop 230-3, Space Technology Division, NASA Ames Research Center, Moffett Field, California 94035

R. S. Ram
Department of Chemistry, University of Arizona, Tucson, Arizona 85721

Peter F. Bernath
Department of Chemistry, University of Waterloo, Waterloo, Ontario, Canada N2L 3G1

C. G. Parsons and D. Galehouse[b)]
Department of Physics, University of Akron, Akron, Ohio 44325

The spectrum of CrH has been reinvestigated in the 9000–15 000 cm^{-1} region using the Fourier transform spectrometer of the National Solar Observatory. The 1-0 and 1-1 bands of the $A\,^6\Sigma^+$-$X\,^6\Sigma^+$ transition have been measured and improved spectroscopic constants have been determined. A value for the 2-0 band origin has been obtained from the band head using estimated spectroscopic constants. These data provide a set of much improved equilibrium vibrational and rotational constants for the $A\,^6\Sigma^+$ state. An accurate description of the A-X transition has been obtained using a multireference configuration interaction approach. The inclusion of both scalar relativity and Cr $3s3p$ correlation are required to obtain a good description of both states. The *ab initio* computed Einstein coefficients and radiative lifetimes are reported. © *2001 American Institute of Physics.* [DOI: 10.1063/1.1377892]

I. INTRODUCTION

CrH was first observed in 1937 by Gaydon and Pearse,[1] who found a complex band near 368 nm. Since then CrH has been studied by several workers[2–6] and a summary of the literature was provided in our previous papers on CrH (Ref. 7) and CrD (Ref. 8). In our most recent high resolution studies of the 0-0 band of CrH[7] and 0-1, 0-0, 1-0, and 1-2 bands of CrD,[8] we obtained much improved molecular constants for the $A\,^6\Sigma^+$ and $X\,^6\Sigma^+$ states of CrH and CrD, and from the observed perturbations we have identified a low-lying $a\,^4\Sigma^+$ state near 11 186 cm^{-1}. These observations have been confirmed in a recent theoretical study by Dai and Balasubramanian.[9]

CrH is a molecule of astrophysical importance. It has already been tentatively identified in the spectra of sunspots[10] and S-type stars[11] and is also found in the spectra of brown dwarfs.[12] Brown dwarfs are substellar objects that lie between the coolest oxygen-rich stars (M-type) and giant planets such as Jupiter. As the surface temperature of an M star drops below approximately 1800 K, metal oxides such as TiO and VO are replaced by metal hydrides such as CrH and FeH. Thus the presence of the 1-0 and 0-0 bands of the $A\,^6\Sigma^+$-$X\,^6\Sigma^+$ transition of CrH are primary markers for L-type brown dwarfs. As the surface temperature drops below approximately 1400 K, metal hydride bands weaken and are replaced by overtone bands of methane and water in the near infrared region in the T-type of brown dwarfs.

An accurate description of the X and A states and the oscillator strengths are required to calculate the molecular opacities used by astronomers to model the spectral energy distribution emitted by brown dwarfs. The ground $X\,^6\Sigma^+$ state of CrH is relatively well characterized through the far infrared[13] and mid infrared[14] laser magnetic resonance measurements. Because there was also some experimental data[5,8] for the A state, our initial plan was to use *ab initio* calculations to compute the transition moment. However, this approach showed that the spectroscopic data for the $A\,^6\Sigma^+$-$X\,^6\Sigma^+$ transition are in need of improvement particularly for the excited vibrational levels of the $A\,^6\Sigma^+$ state. Thus a joint computational/experimental approach is used.

In the present work we have remeasured the spectra of the 1-0 and 1-1 bands of the $A\,^6\Sigma^+$-$X\,^6\Sigma^+$ transition of CrH and have obtained an improved set of constants for the $v'=1$ vibrational level of the $A\,^6\Sigma^+$ state. The band origin for the 2-0 band has been determined by fitting the band head position using extrapolated rotational constants for the $v'=2$ level. In the ground state all of the available data for $v''=0$, 1, and 2 were combined to determine a set of improved vibrational and rotational equilibrium constants. High level *ab initio* calculations were performed for the X and A states, which are compared with experiment. The calculations also yielded an accurate transition dipole moment.

II. EXPERIMENTAL APPROACH

The spectrum of CrH in the 9000–15 000 cm^{-1} region was recorded using the 1-m Fourier transform spectrometer associated with the McMath–Pierce telescope of the Na-

---

[a)]Electronic mail: bauschli@pegasus.arc.nasa.gov
[b)]Current address: 15764 Galehouse Road, Doylestown, OH 44230.

tional Solar Observatory at Kitt Peak. The bands were excited using two kinds of sources, a hollow cathode lamp and a microwave discharge lamp. In the hollow cathode experiment the molecules were formed by flowing a mixture of 2.8 Torr of Ne and about 100 mTorr of H_2 through a Cr hollow cathode lamp, which was operated at 460 V and 765 mA current. The spectrometer was operated with a GG495 red pass filter and midrange photodiode detectors. In this experiment 19 scans were coadded at $0.02\,\mathrm{cm}^{-1}$ resolution in about 2 h of integration.

In the microwave-discharge experiment the chromium was introduced as a volatile compound and reacted in the flow tube. Approximately 15% hydrogen mixed with helium carrier gas was admitted into the feed line. A small amount of CrO_2Cl_2 was vaporized into the mixed stream of gas. Under these conditions, the chromium is reduced preferentially to CrH during excitation. The pressure was adjusted to 20–30 Torr with the aid of a needle valve on the pump line. The chromium concentration was adjusted by controlling the chamber temperature or with a controlled bypass. The mixture was carried through a 11 mm i.d. quartz discharge tube within the microwave cavity. The flow rate affects the time allowed for the reaction and also the Doppler linewidth because of the cooling effect of rapid flows. The operating parameters are not particularly sensitive and a strong CrH spectrum was obtained easily. The spectrum was taken at Kitt Peak National Observatory on May 21, 1985.

The spectra were measured using a data reduction program called PC-DECOMP and the line positions were obtained by fitting a Voigt line shape function to each spectral feature. The hollow cathode spectrum was calibrated using the measurements of Ne atomic lines by Palmer and Engleman[15] while the microwave-excited spectra were calibrated by transferring the calibration from the hollow cathode spectra to the microwave-excited spectra using common lines. The absolute accuracy of the wave number scale is expected to be of the order of $0.001\,\mathrm{cm}^{-1}$ while the precision of lines is expected to vary from 0.002 to $0.004\,\mathrm{cm}^{-1}$ depending on their intensity, signal-to-noise ratio, and blending.

III. COMPUTATIONAL METHODS

The X and A states are treated using the multiconfigurational self-consistent-field/multireference configuration interaction approach, MCSCF/MRCI. The MRCI calculations use all MCSCF configurations as reference configurations. In many calculations, internal contraction[16] (IC) is used to limit the size of the calculations. The importance of higher excitations is estimated using the multireference analog of the Davidson correction. In most calculations only the Cr $3d$ and $4s$ and H $1s$ electrons are correlated. The calculations including Cr $3s$ and $3p$ correlation are denoted "$+3s3p$." Scalar relativistic effects are included using the one-electron Douglas Kroll (DK) approach.[17]

Several choices of active space are considered. In the calculations labeled MCSCF, MRCI, IC-MRCI, DK-MRCI, and IC-MRCI$+3s3p$ the active space in the MCSCF and MRCI calculations includes the Cr $3d$, $4s$, $4p\sigma$, and H $1s$ orbitals. In these calculations, the MCSCF calculations are actually a complete active space SCF (CASSCF) calculation

as all distributions of the active electrons in the active orbitals are used. In C_{2v} symmetry there are five active a_1 orbitals and one active orbital in the b_1, b_2, and a_2 symmetries, which we denote as (4111). In the MCSCF calculations, each component of the $3d\pi$ and $3d\delta$ orbitals has an occupation of essentially 1.0 electrons, thus this calculation effectively corresponds to all distributions of three electrons in the Cr $3d\sigma$, $4s$, $4p\sigma$, and H $1s$ orbitals. This calculation can describe bonding from both the ^7S and ^5D states of Cr. The "$+dd'$" calculations indicate the Cr d-d' correlation has been included by adding a $3d'$ orbital to the active space, yielding a (7222) active space. To reduce the size of the calculation, we restrict the configurations to those with four electrons in the $3d\pi$, $3d\pi'$, $3d\delta$, and $3d\delta'$ orbitals. The "$+p\pi$" indicates that the Cr $4p\pi$ orbital has been included in the active space, thus yielding a (5221) active space; to prevent the added orbitals from becoming d correlating in character, we include only those configurations with four electrons in the $3d\pi$ and $3d\delta$ orbitals. In the calculation labeled IC-MRCI$+p\pi dd'$, the active space includes the Cr $3d$, $3d'$, $4s$, and $4p$ orbitals and the hydrogen $1s$ orbital, i.e., a (7332) active space. There are no restrictions on the configurations, and thus this MCSCF is actually a CASSCF calculation.

Three basis sets are used in this work. The set labeled "ANO" is the averaged atomic natural orbital set[18] for Cr, which can be described as $(20s15p10d6f4g)/[7s6p4d3f2g]$, and for hydrogen, is the augmented-correlation-consistent polarized-valence triple zeta (aug-cc-pVTZ) set.[19,20] The ANO+ set starts from this set and uncontracts an additional s, p, and d primitive, as well as adding an additional diffuse s, p, and d function to the Cr basis set; the hydrogen basis set is the aug-cc-pV quadruple zeta set. The diffuse Cr functions are even tempered with a β of 2.5. The set labeled "GEN" uses the hydrogen aug-cc-pVTZ set, but recontracts the Cr ANO primitive basis set. The s, p, and d primitives are contracted based on an SCF calculation of the ^7S state of a Cr atom. The inner $16s$ primitives are contracted to three functions and the outermost four are uncontracted, the inner $10p$ primitives are contracted to two functions and the outermost five are uncontracted, and the inner $5d$ primitives are contracted to one function and the outermost five are uncontracted. The f and g sets are taken from the ANO set. The GEN basis can be described as $(20s15p10d6f4g)/[7s7p6d3f2g]$, and this contraction is suitable for the study of Cr $3s3p$ correlation.

In the preliminary work, the potentials near r_e are studied and ω_e is computed using a parabolic function in r and $1/r$, which agree with each other to better than $3\,\mathrm{cm}^{-1}$. In the final phase, complete potentials are computed and the vibrational levels are determined numerically. Using the separations between the lowest three levels, we computed ω_e and $\omega_e x_e$. These potentials along with the computed electronic transition moments are used to compute the radiative lifetimes and Einstein A values.

The MCSCF/IC-MRCI calculations are performed using MOLPRO[21] while the MCSCF/MRCI calculations are performed using MOLECULE-SWEDEN.[22] The DK integrals are
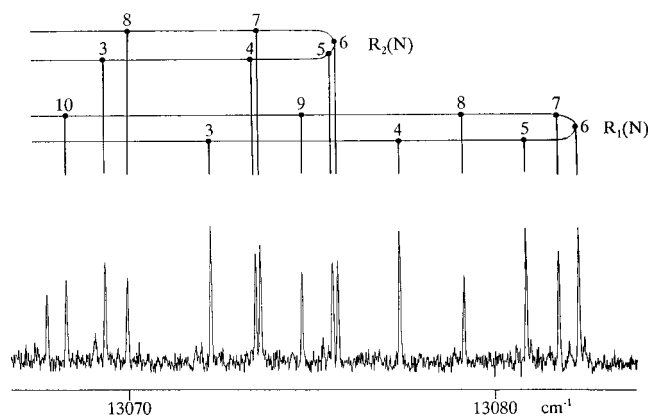
FIG. 1. The 1-0 band head of the $A\ ^6\Sigma^+$-$X\ ^6\Sigma^+$ transition of CrH.

computed using a modified version of the program written by Hess.

IV. ANALYSIS AND DISCUSSION OF EXPERIMENT

The spectrum of the 1-0 band of the $A\ ^6\Sigma^+$-$X\ ^6\Sigma^+$ transition observed in the microwave-excited spectrum, particularly for low J lines, is stronger than that obtained in the hollow cathode experiment. In part, this is because the microwave discharge source is cooler than the hollow cathode lamp. Both of these spectra, when used simultaneously, were very helpful in identifying the molecular lines belonging to CrH. The line positions of 1-0 and 1-1 bands provided by O'Connor[2] at lower resolution were also helpful in the line identification. No bands involving the $v=2$ vibrational level of the $A\ ^6\Sigma^+$ state were observed. A part of the 1-0 band from the microwave-excited spectrum is provided in Fig. 1, where a few lines near the R_1 and R_2 heads have been marked. It is found that the lines of higher energy spin components (F_5 and F_6) are much weaker than the lines of the lower energy spin components (F_1 and F_2). In fact only a few lines of the F_5 spin components were identified in our spectra while no lines could be identified in the F_6 spin component. The line identification in the 1-0 band was accomplished using lower state combination differences obtained from the previous analysis of the 0-0 band of CrH[7] while the lines in the 1-1 band were identified by comparing the upper state combination differences from the 1-0 and 1-1 bands. The line positions for the 1-0 and 1-1 bands are presented in the Supplementary Material Section of Ref. 23 as E-PAPS document files. The line positions of the 0-0, 1-0, and 1-1 bands were fitted simultaneously with the usual N^2 Hamiltonian as given by Brown and Milton[24] with matrix elements provided by Gordon and Merer.[25] A complete listing of matrix elements with some additional parameters such as H, L, γ_H, and γ_L was tabulated in our previous paper on CrH.[7] The final fits were made in two parts. First the hyperfine-free pure rotational transitions[26] and the hyperfine-free vibration–rotation line positions calculated using the constants of Lipus *et al.*[14] were included in a fit along with our previous 0-0 lines of the $A\ ^6\Sigma^+$-$X\ ^6\Sigma^+$ transition and all available ground state combination differences. The constants T_v, B_v, D_v, H_v, γ_v, γ_{Dv}, λ_v, λ_{Dv}, θ_v, and γ_{sv}

were varied in the ground state with T_0 fixed to a value of 0.0. The parameters H_v, θ_v, and γ_{sv} were not determined for the $v=1$ and 2 vibrational levels of the ground state. The γ_{Dv} constants were needed for $v''=1$ and 2 vibrational levels and were fixed at the values reported by Lipus *et al.*[14] For $v'=0$, additional higher order parameters are also required in order to obtain a satisfactory fit. In the second fit the 1-0 and 1-1 lines were added and only the $v'=1$ constants were varied. The lines of the F_6 spin components as well as the high J lines of the other spin components that were observed by O'Connor[2] were used but with reduced weights. The H_v, L_v, γ_{Lv}, θ_v, θ_{Dv}, and γ_{sDv} constants were not determined for the $v'=1$ vibrational level of the $A\ ^6\Sigma^+$ state. It is found that $v'=1$ is affected by several perturbations as can be seen from the observed-calculated differences for the lines of the 1-0 and 1-1 bands. The perturbations show no clear patterns and we are unable to draw any conclusion about the nature of the perturbing state (or states). In our previous work on CrH, the observed localized perturbations in the 0-0 band led us to identify the $a\ ^4\Sigma^+$ state lying just below the $A\ ^6\Sigma^+$ state. More than one state may be responsible for the extensive perturbations observed in bands with $v'=1$. The molecular constants for the ground and excited states are provided in Table I.

The rotational constants obtained for the $v=0$ and 1 vibrational levels of the $A\ ^6\Sigma^+$ state have been used to derive the equilibrium rotational constants B_e and α_e. Because the term energy position of the $v'=2$ level of the $A\ ^6\Sigma^+$ state is necessary to derive the equilibrium vibrational constants, we have used the 2-0 band head position ($14\,510.6\ cm^{-1}$) as reported by Kleman and Uhler[4] to determine the band origin of the 2-0 band. We have fixed the extrapolated rotational constants for the $v'=2$ level and the known rotational constants for the $v''=0$ level in our fitting program and changed the band origin in such a way that the calculated band head position matches the observed band head position. The 2-0 band origin of $T_2=14\,468.6\ cm^{-1}$ obtained in this manner is expected to have a precision of about $\pm 0.5\ cm^{-1}$. The equilibrium vibrational constants of $\omega_e=1524.80(50)\ cm^{-1}$ and $\omega_e x_e=22.28(25)\ cm^{-1}$ were obtained for the $A\ ^6\Sigma^+$ state using the experimental T_0 and T_1 values and the calculated T_2 value. The rotational constants of Table I provide the equilibrium rotational constants of $B_e=5.342\,675(48)\ cm^{-1}$ and $\alpha_e=0.141\,349(88)\ cm^{-1}$ for the $A\ ^6\Sigma^+$ state. An experimental bond length of $r_e=1.786\,485\,0(80)$ Å has been obtained for the $A\ ^6\Sigma^+$ state using the equilibrium rotational constant. The ground state equilibrium constants were also determined using the constants for the $v''=0$, 1, and 2 vibrational levels (Table I). A complete set of the equilibrium constants for the ground and excited state is provided in Table II.

It is interesting to compare our experimental values to those obtained in our theoretical calculations. The experimental ground state values of $\omega_e=1656.051\,15(54)\ cm^{-1}$, $\omega_e x_e=30.491\,23(26)\ cm^{-1}$, and $r_e=1.655\,411\,1(57)$ Å are in excellent agreement with the theoretical values of $\omega_e=1653.6\ cm^{-1}$, $\omega_e x_e=31.0\ cm^{-1}$, and $r_e=1.654$ Å obtained using the corrected potential as described in detail in the text (theoretical part). Similarly the excited state experimental values of $\omega_e'=1524.80(50)\ cm^{-1}$, $\omega_e x_e'=22.28(25)\ cm^{-1}$,

TABLE I. Rotational constants (in cm^{-1}) for the $X\,^6\Sigma^+$ and $A\,^6\Sigma^+$ states of CrH.

Constants[a]	$X\,^6\Sigma^+$			$A\,^6\Sigma^+$	
	$v=0$	$v=1$	$v=2$	$v=0$	$v=1$
T_v	0.0	1595.068 70(14)	3129.154 95(48)	11 552.684 16(75)	13 032.9233(39)
B_v	6.131 737 4(18)	5.950 759 3(96)	5.769 783(84)	5.272 000(18)	5.130 651(86)
$D_v\times10^4$	3.489 22(24)	3.440 73(88)	3.385(24)	2.5458(12)	1.6269(43)
$H_v\times10^9$	12.471(27)			4.77(22)	
$L_v\times10^{12}$				2.18(14)	
γ_v	0.050 362 9(64)	0.046 454(14)	0.042 577(29)	1.302 076(70)	1.429 85(20)
$\gamma_{Dv}\times10^4$	$-0.029\ 03(62)$	-0.0205[b]	-0.0755[b]	$-1.5431(46)$	$-4.303(20)$
$\gamma_{Hv}\times10^7$				0.800(20)	$-9.49(15)$
$\gamma_{Lv}\times10^{11}$				$-2.45(15)$	
λ_v	0.232 820 6(56)	0.224 003(49)	0.215 132(98)	1.575 53(22)	1.5463(12)
$\lambda_{Dv}\times10^4$	$-0.0966(54)$	0.161(31)	0.268(60)	$-8.360(32)$	4.28(11)
$\theta_v\times10^3$	$-7.85(30)$			2.98(13)	
$\theta_{Dv}\times10^4$				$-1.017(20)$	
$\gamma_{sv}\times10^3$	0.005 27(89)			0.9182(96)	3.962(22)
$\gamma_{sDv}\times10^6$				6.380(71)	

[a]Numbers in parentheses are one standard deviation in the last digits.
[b]Fixed value, see text for details.

and $r_e'=1.786\ 485\ 0(80)$ Å are also in excellent agreement with our theoretical values of $\omega_e'=1525.2\ cm^{-1}$, $\omega_e x_e' =23.0\ cm^{-1}$, and $r_e'=1.765$ Å. Significantly different values of $\omega_e'=1515\ cm^{-1}$ and $\omega_e x_e'=21.5\ cm^{-1}$ were obtained by Kleman and Uhler[5] for the $A\,^6\Sigma^+$ state from the analysis of their lower resolution spectra.

V. COMPUTATIONAL RESULTS AND DISCUSSION

The $X\,^6\Sigma^+$ state is derived mostly from the $^7S(3d^54s^1)$ ground state of Cr, which has formed a $4s$-$1s$ bond with hydrogen. The first excited state of Cr $[^5S(3d^54s^1)]$ also yields a $^6\Sigma^+$ state, but it is not expected to be strongly bound. However, the second excited state of Cr, $^5D(3d^44s^2)$, can bond to hydrogen by $4s4p$ hybridization, which gives rise to the $A\,^6\Sigma^+$ state. In truth, the X and A states are somewhat mixed in character, with the X state being derived mostly from ^7S but with some ^5D mixed in and the A state from mostly Cr ^5D. Since the states are derived from Cr occupations with a different number of d electrons, high levels of theory are required to obtain an equivalent description of both states. A slight further complication is curve crossing at large r for the A state due to the Cr ^5S state lying below the ^5D.

We first consider the results obtained by our approaches for the X state, which are summarized in Table III. The

TABLE II. Equilibrium constants (in cm^{-1}) for the $X\,^6\Sigma^+$ and $A\,^6\Sigma^+$ states of CrH.

Constants	$X\,^6\Sigma^+$	$A\,^6\Sigma^+$
$\Delta G_{1/2}$	1595.068 70(14)	1480.2391(40)
B_e	6.222 226 42(10)	5.342 675(48)
α_e	0.180 978 08(18)	0.141 349(88)
r_e (Å)	1.655 411 1(57)	1.786 485 0(80)
ω_e	1656.051 15(54)	1524.80(50)[a]
$\omega_e x_e$	30.491 23(26)	22.28(25)[b]

[a]Numbers in parentheses are one standard deviation in the last digits.
[b]See text for details.

MCSCF yields an r_e that is too long and ω_e and D_0 values that are too small. Adding more extensive correlation dramatically improves the results, but the IC-MRCI/ANO and IC-MRCI+Q/ANO results are only in reasonable agreement with experiment. Using the GEN basis set yields essentially the same results as the ANO set, while expanding the basis set, i.e., ANO+, makes only a small change. The MRCI and IC-MRCI results are similar, showing that internal contraction is not the cause for the disagreement with experiment. Increasing the active space, the $+p\pi$ or $+dd'$ approaches, makes only a small improvement. Adding Cr $3s3p$ correlation makes a bigger change than improving the active space, but the r_e is still too long and ω_e is still too small. Accounting for the scalar relativistic effects, using the DK approach, has a significant effect on the computed spectroscopic con-

TABLE III. The X state spectroscopic constants as a function of level of theory.

Method	Basis	r_e(Å)	ω_e(cm^{-1})	D_0(eV)
MCSCF	ANO	1.721	1525	1.39
IC-MRCI	ANO	1.684	1581	2.06
IC-MRCI+Q	ANO	1.685	1577	2.16
IC-MRCI	ANO+	1.681	1586	2.09
IC-MRCI+Q	ANO+	1.682	1584	2.18
IC-MRCI+dd'	ANO	1.679	1593	2.08
IC-MRCI+Q+dd'	ANO	1.679	1596	2.13
IC-MRCI+$p\pi$	ANO	1.683	1586	2.06
IC-MRCI+Q+$p\pi$	ANO	1.683	1582	2.16
IC-MRCI	GEN	1.683	1581	2.04
IC-MRCI+Q	GEN	1.684	1577	2.16
IC-MRCI+$3s3p$	GEN	1.673	1595	1.98
IC-MRCI+Q+$3s3p$	GEN	1.670	1601	2.16
MRCI	GEN	1.681	1585	2.07
MRCI+Q	GEN	1.682	1581	2.17
DK-MRCI	GEN	1.669	1631	2.15
DK-MRCI+Q	GEN	1.669	1628	2.17
Experiment		1.655[a]	1656[a]	1.93 ± 0.07[b]

[a]This work.
[b]Reference 27.

TABLE IV. The *A* state spectroscopic constants as a function of level of theory.

Method	Basis	r_e(Å)	*A* state ω_e(cm^{-1})	T_e(cm^{-1})	TM[a]
MCSCF	ANO	1.876	1337	8126	
IC-MRCI	ANO	1.782	1516	10 611	0.7101
IC-MRCI+Q	ANO	1.774	1537	11 088	
IC-MRCI	ANO+	1.779	1521	10 517	0.7194
IC-MRCI+Q	ANO+	1.771	1542	10 993	
IC-MRCI+dd'	ANO	1.776	1525	10 796	0.7149
IC-MRCI+Q+dd'	ANO	1.774	1531	10 925	
IC-MRCI+$p\pi$	ANO	1.781	1520	10 628	0.6986
IC-MRCI+Q+$p\pi$	ANO	1.773	1538	11 137	
IC-MRCI+$p\pi dd'$	ANO				0.6943
IC-MRCI	GEN	1.780	1519	10 513	0.7183
IC-MRCI+Q	GEN	1.772	1539	10 990	
IC-MRCI+$3s3p$	GEN	1.778	1506	10 513	0.7205
IC-MRCI+Q+$3s3p$	GEN	1.764	1514	11 270	
MRCI	GEN	1.779	1515	10 478	0.7339
MRCI+Q	GEN	1.771	1535	10 946	
DK-MRCI	GEN	1.783	1494	10 362	0.7308
DK-MRCI+Q	GEN	1.775	1517	10 758	
Experiment		1.786[b]	1525[b]	11616[b]	

[a]The dipole transition moment, in a.u., at 1.69 Å.
[b]Present work.

stants, and we obtain our best agreement with experiment. However, even at this level, the r_e is still too long and ω_e is still too small.

While the calculation of D_0 is not the main focus of this work, we note that essentially all of our computed MRCI values are larger than experiment.[27] We suspect that the +Q values are more accurate than those without the correction, and the +Q values suggest a D_0 value of about 2.15 eV. The smallest value computed is 1.98 eV at the IC-MRCI+$3s3p$ level, but this approach has a large +Q effect, which is consistent with correlating 15 electrons. We therefore believe that it is better to take the IC-MRCI as our lower bound of 2.06 eV, leading to our best theoretical estimate of 2.15 ±0.1 eV for the D_0 of CrH.

In Table IV we summarize the results obtained for the *A* state. As expected the MCSCF results do not agree well with experiment, and more extensive correlation must be added. While the IC-MRCI r_e is in good agreement with experiment, the ω_e and T_e values are too small. The IC-MRCI+Q improves T_e, but degrades r_e and ω_e. The effect of the +Q correction is much larger than for the *X* state. The ANO, GEN, and ANO+ results are sufficiently similar so that basis set incompleteness does not appear to be a problem, nor does internal contraction, as measured by the difference between the IC-MRCI and MRCI results using the GEN basis. Adding the d-d' correlation to the active space reduces the size of the +Q effect and the ω_e is now in better agreement with experiment. Adding $3s3p$ correlation in the IC-MRCI +$3s3p$ calculation yields ω_e and T_e values that are too small. The +Q improves ω_e and T_e values, but results in an r_e value that is too small. The DK-MRCI+Q gives reasonable agreement with experiment for r_e and ω_e, but its T_e value is too small.

We have computed the *A*-*X* transition moment at several *r* values for most of the methods considered in this work.

The moment is about 1.3 a.u. at 1 Å and decreases in a nearly linear manner until about 2.5 Å. Due to the avoided crossing in the A state, the moment changes dramatically near 3 Å (see Fig. 2), and this change depends strongly on the level of theory. Luckily, the region of the change in the transition moment is not in the Franck–Condon region for the v' less than or equal to 3, and therefore it has only a very small affect on the reported A values. The change in the
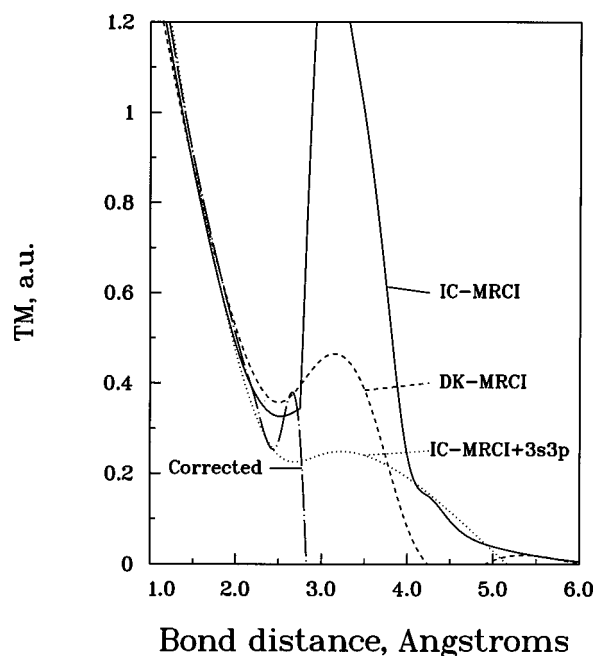

FIG. 2. The computed *A*-*X* transition moment for three levels of theory and the corrected transition moment (see text).

TABLE V. Summary of the computed spectroscopic constants using full potentials.

Method/Basis	r_e(Å)	D_0(eV)	ω_e(cm^{-1})	$\omega_e x_e$(cm^{-1})	
		X state			
ICMRCI/ANO	1.684	2.06	1580.3	30.2	
ICMRCI+Q/ANO	1.685	2.16	1575.8	29.6	
ICMRCI+$p\pi$/ANO	1.683	2.06	1585.2	29.9	
ICMRCI+Q+$p\pi$/ANO	1.683	2.16	1580.2	29.5	
ICMRCI+dd'/ANO	1.679	2.08	1592.6	30.3	
ICMRCI+Q+dd'/ANO	1.679	2.13	1595.7	30.0	
DK-MRCI/GEN	1.669	2.15	1631.1	30.7	
DK-MRCI+Q/GEN	1.669	2.17	1628.4	30.6	
ICMRCI+$3s3p$/GEN	1.673	1.98	1595.2	30.9	
ICMRCI+Q+$3s3p$/GEN	1.670	2.16	1601.3	30.1	
Corrected[a]	1.654	2.17	1653.8	31.0	
Experiment	1.655[b]	1.93±0.07[c]	1656.05[b]	30.49[b]	

Method/Basis	r_e(Å)	ω_e(cm^{-1})	$\omega_e x_e$(cm^{-1})	A(s^{-1})	Error T_0(cm^{-1})
		A state			
ICMRCI/ANO	1.782	1516.8	22.8	0.111(+7)	972.3
ICMRCI+Q/ANO	1.774	1537.4	23.7	0.116(+7)	483.5
ICMRCI+$p\pi$/ANO	1.781	1520.5	22.3	0.108(+7)	955.8
ICMRCI+Q+$p\pi$/ANO	1.773	1538.1	23.3	0.113(+7)	435.7
ICMRCI+dd'/ANO	1.776	1525.7	23.6	0.116(+7)	789.3
ICMRCI+Q+dd'/ANO	1.774	1531.8	24.0	0.117(+7)	658.5
DK-MRCI/GEN	1.783	1494.5	22.8	0.112(+7)	1256.8
DK-MRCI+Q/GEN	1.775	1517.5	23.8	0.117(+7)	849.0
ICMRCI+$3s3p$/GEN	1.778	1506.4	21.8	0.112(+7)	1081.9
ICMRCI+Q+$3s3p$/GEN	1.764	1544.6	22.9	0.120(+7)	310.2
Corrected[a]	1.765	1525.2	23.0	0.120(+7)	656.8
Experiment[b]	1.7865	1524.80	22.28		

[a]See text for definition.
[b]Present work.
[c]Reference 27.

transition moment with level of theory at 1.69 Å is representative of the linear region and therefore we give the moment at this r value in Table IV. While it is too expensive to perform IC-MRCI+$p\pi dd'$ calculations at many r values, it is possible to compute the transition moment at this level at 1.69 Å. We first note that the computed transition moments are not strongly affected by the different levels of theory. It is interesting that the inclusion of the Cr$4p\pi$ orbitals in the active space decreases the moment somewhat, which is supported by the IC-MRCI-$p\pi dd'$ calculation. The calculations using the GEN and ANO+ basis sets suggest that basis set improvements will increase the moment. The difference between the MRCI and IC-MRCI calculations show that eliminating the internal contraction increases the computed transition moment slightly. We conclude that our computed transition moments are accurate because the values vary only slightly with level of theory.

On the basis of the calibration calculations, it appears that one must account for both $3s3p$ correlation and scalar relativistic effects. The results also suggest that using a very large active space would be ideal. Unfortunately we are unable to include all of these effects in a calculation for which it is practical to compute an entire surface. We have therefore computed full potentials for a subset of the methods considered in Tables III and IV, and the results are given in Table V. Following Partridge and Schwenke,[28] we tried merging these potentials into one that accounts for all of these effects.

Our best derived potential corrects the DK-MRCI+Q potential for the $3s3p$ correlation, i.e.,

$$E(\text{corrected}) = E(\text{DK-MRCI+Q}) + E(\text{ICMRCI+Q} + 3s3p) - E(\text{IC-MRCI+Q}).$$

For the X state, this potential yields excellent agreement with experiment, excluding the somewhat uncertain D_0 value. The same correction for the A state yields very good results for ω_e and $\omega_e x_e$, but the r_e value is a bit short, see Table V. We should note that the difference between these A state results and the older values[5] was part of the motivation for the new experimental analysis of the A state. While the corrected potential did detect some problem with the older spectroscopic constants, it is far from perfect, the A state r_e is too short and T_0 is too small.

We derive a corrected transition moment in a manner analogous to the potentials, namely

$$\text{TM(corrected)} = \text{TM(DK-MRCI)} + \text{TM(ICMRCI} + 3s3p) - \text{TM(IC-MRCI)}.$$

This moment has a small bump at about 2.6 Å and becomes negative at Cr–H distances larger than 2.8 Å, see Fig. 2. Since these features may be nonphysical, we also test three modified versions: (1) where the negative values are removed by setting the transition moment to zero at distances

TABLE VI. Einstein coefficients (in s^{-1}) for A-X transition and A state radiative lifetimes computed using the corrected potentials.

$A_{v'v''}$	Value	$A_{v'v''}$	Value
A_{00}	0.120(+7)	A_{22}	0.270(+6)
A_{01}	0.134(+6)	A_{23}	0.211(+6)
A_{02}	0.102(+4)	A_{24}	0.198(+4)
A_{10}	0.624(+6)	A_{30}	0.852(+5)
A_{11}	0.584(+6)	A_{31}	0.445(+6)
A_{12}	0.192(+6)	A_{32}	0.640(+6)
A_{13}	0.180(+4)	A_{33}	0.116(+6)
A_{20}	0.242(+6)	A_{34}	0.211(+6)
A_{21}	0.730(+6)	A_{35}	0.146(+4)
Radiative lifetimes			
v	$\tau(\mu s)$	v	$\tau(\mu s)$
0	0.75	2	0.69
1	0.71	3	0.67

larger than 2.8 Å, (2) where the bump and negative regions are removed by connecting, with a spline function, the computed moment at $r(\text{Cr–H}) = 2.4$ Å with a value of zero at $r(\text{Cr–H}) = 4.5$ Å, and (3) where the bump and negative regions are removed by connecting the computed moment at $r(\text{Cr–H}) = 2.4$ Å with a value of zero at $r(\text{Cr–H}) = 2.8$ Å. For $v' \leq 3$ and $v'' \leq 5$, the A values are essentially independent of these modifications to the transition moment; our reported A values are computed using the transition moment where the value is set to zero for $r(\text{Cr–H})$ greater than 2.8 Å.

In Table V we report A_{00} values obtained using the computed and corrected potentials. One observation is that the A_{00} values do not vary significantly with level of theory, ranging from 0.108(+7) to 0.120(+7). We therefore conclude that our computed value is probably accurate to 10%–20%.

In Table VI we report additional A values and some radiative lifetimes for the corrected potentials. The small difference in the r_e values for the X and A states results in a few large A values for each v' level. The radiative lifetimes vary by even less with level of theory than A_{00}, and so we expect these to be even more accurate. The radiative lifetimes vary slightly with v'.

VI. CONCLUSIONS

We have reinvestigated the $A\ ^6\Sigma^+$-$X\ ^6\Sigma^+$ transition in CrH. The 1-0 and 1-1 bands have been measured and improved spectroscopic constants have been determined. A value for the 2-0 band origin has been obtained from the band head using estimated spectroscopic constants. These data provide a set of much improved equilibrium vibrational and rotational constants for the $A\ ^6\Sigma^+$ state.

We have studied the X and A states of CrH and found that high levels of theory are required to obtain a good de-

scription of the states. Scalar relativistic effects are found to be important. Cr $3s3p$ correlation is also important. The computed Einstein A values and radiative lifetimes do not vary strongly with level of theory, leading us to conclude that our computed values are accurate. The calculations also suggest that the D_0 of CrH is slightly larger than the most recent experimental value.

[1] A. G. Gaydon and R. W. B. Pearse, Nature (London) **140**, 110 (1937).
[2] S. O'Connor, J. Phys. B **2**, 541 (1969).
[3] R. E. Smith, Proc. R. Soc. London, Ser. A **332**, 113 (1973).
[4] B. Kleman and B. Liljeqvist, Ark. Fys. **9**, 345 (1955).
[5] B. Kleman and U. Uhler, Can. J. Phys. **37**, 537 (1959).
[6] S. O'Connor, Proc. R. Ir. Acad., Sect. A, Math. Astron. Phys. Sci. **9**, 95 (1967).
[7] R. S. Ram, C. N. Jarman, and P. F. Bernath, J. Mol. Spectrosc. **161**, 445 (1993).
[8] R. S. Ram and P. F. Bernath, J. Mol. Spectrosc. **172**, 91 (1995).
[9] D. Dai and K. Balasubramanian, J. Mol. Spectrosc. **161**, 455 (1993).
[10] O. Engvold, H. Wöhl, and J. W. Brault, Astron. Astrophys., Suppl. Ser. **42**, 209 (1980).
[11] B. Lindgren and G. S. Olofsson, Astron. Astrophys. **84**, 300 (1980).
[12] J. D. Kirkpatrick, F. Allard, T. Bida, B. Zuckerman, E. E. Becklin, C. Chabrier, and I. Baraffe, Astrophys. J. **519**, 834 (1999).
[13] S. M. Corkery, J. M. Brown, S. P. Beaton, and K. M. Evenson, J. Mol. Spectrosc. **149**, 257 (1991).
[14] K. Lipus, E. Bachem, and W. Urban, Mol. Phys. **73**, 1041 (1991).
[15] B. A. Palmer and R. Engleman, *Atlas of the Thorium Spectrum* (Los Alamos National Laboratory, Los Alamos, 1983).
[16] H.-J. Werner and P. J. Knowles, J. Chem. Phys. **89**, 5803 (1988); P. J. Knowles and H.-J. Werner, Chem. Phys. Lett. **145**, 514 (1988).
[17] B. A. Hess, Phys. Rev. A **33**, 3742 (1986).
[18] C. W. Bauschlicher, Theor. Chim. Acta **92**, 183 (1995).
[19] T. H. Dunning, J. Chem. Phys. **90**, 1007 (1989).
[20] R. A. Kendall, T. H. Dunning, and R. J. Harrison, J. Chem. Phys. **96**, 6796 (1992).
[21] MOLPRO is a package of *ab initio* programs written by H.-J. Werner and P. J. Knowles, with contributions from J. Almlöf, R. D. Amos, A. Berning *et al.*, The closed shell CCSD program is described in C. Hampel, K. Peterson, and H. J. Werner, Chem. Phys. Lett. **190**, 1 (1992).
[22] MOLECULE-SWEDEN is an electronic structure program written by J. Almlöf, C. W. Bauschlicher, M. R. A. Blomberg, D. P. Chong, A. Heiberg, S. R. Langhoff, P.-Å. Malmqvist, A. P. Rendell, B. O. Roos, P. E. M. Siegbahn, and P. R. Taylor.
[23] See AIP Document No. E-JCPSA6-115-034125 for a table containing the line list. This document may be retrieved via the EPAPS homepage (http://www.aip.org/pubservs/epaps.html) or from ftp.aip.org in the directory /epaps/. See the EPAPS homepage for more information.
[24] J. M. Brown and D. J. Milton, Mol. Phys. **31**, 409 (1978).
[25] R. M. Gordon and A. J. Merer, Can. J. Phys. **56**, 642 (1980).
[26] J. M. Brown (private communication), see Ref. 7.
[27] Y.-M. Chen, D. E. Clemmer, and P. B. Armentrout, J. Chem. Phys. **98**, 4929 (1993).
[28] H. Partridge and D. W. Schwenke, J. Chem. Phys. **106**, 4618 (1997).